

DESY SR-79/22  
October 1979

Eigentum der Property of	<b>DESY</b>	Bibliothek library
Zugang: Accessions:	18. OKT. 1979	
Leihfrist: Loan period:	7	Tage days

Anisotropic EXAFS in GeS

by

P. Rabe, G. Tolkiehn, and A. Werner

*Institut für Experimentalphysik der Universität Kiel*

To be sure that your preprints are promptly included in the  
HIGH ENERGY PHYSICS INDEX ,  
send them to the following address ( if possible by air mail ) :

DESY  
Bibliothek  
Notkestrasse 85  
2 Hamburg 52  
Germany

DESY DR-79/28  
October 1978

Anisotropic EXAFS in GeS

P. Rabe, G. Tolkiehn, and A. Werner

Institut für Experimentalphysik, Universität Kiel, Kiel, Germany (FRG)

Abstract

Polarized X-rays of the Deutsches Elektronen-Synchrotron have been used to measure the anisotropic absorption of a GeS single crystal at the Ge K-edge. The orientation dependent radial structure functions which have been calculated from the extended X-ray absorption fine-structure (EXAFS) are used to evaluate the three-dimensional arrangement of the atoms in the crystal. An excellent agreement of these results with X-ray diffraction data is observed.

1. Introduction

The investigation of the extended X-ray absorption fine-structure is developing to a standard routine for the evaluation of local geometrical structures (Stern 1974, Lytle et al 1975, Stern et al 1975, Martens et al 1978, Rabe 1978). EXAFS is caused by a superposition of the outgoing photoelectron wave with parts of it backscattered elastically from the atoms surrounding the absorbing atoms. Relative to the polarization vector of the X-rays the electrons are emitted from the central atom into preferred directions which depend on the final state symmetry. For polycrystalline or amorphous samples this angular dependence averages out. In this case only isotropic radial structure functions can be studied. In anisotropic samples such as single crystals with lower than cubic symmetry the contributions to EXAFS from different atoms depend on the orientation of the sample relative to the electric vector of the X-rays. Therefore the probing of bond lengths, coordination numbers, Debye-Waller-Factors, and the type of scattering atoms in selected directions in the crystal becomes feasible. Only few examples are known in which one has taken advantage of this effect for structural analysis (Heald and Stern 1977, Heald and Stern 1978, Brown et al 1977).

For structural investigations utilizing the anisotropy of the EXAFS an intense light source with a high degree of polarization is favourable. Since high energy electron accelerators are available as light sources in the X-ray region many experimental difficulties due to low intensities of the bremsstrahlung of conventional X-ray tubes have been

overcome. Moreover the synchrotron radiation is well known to be linearly polarized in the plane of the electron orbit. Therefore electron-synchrotrons and storage rings are ideal sources for polarization dependent experiments in the X-ray region.

In this paper we report the analysis of the anisotropic absorption in a GeS single crystal which forms a layered structure with orthorhombic unit cell (Wyckoff 1968, Bissert and Hesse 1978) with  $a = 4.297 \text{ \AA}$ ,  $b = 10.470 \text{ \AA}$ ,  $c = 3.641 \text{ \AA}$ . This crystal easily cleaves in the a-c-plane. With the polarization vector  $\hat{c}$  in the a-c-plane an angular dependence of the EXAFS is expected by rotating the crystal around the b-axis, which is kept parallel to the X-ray beam.

In this configuration the angular dependence can be measured without variation of the effective sample thickness. Such a variation would pretend a polarization dependence of the EXAFS amplitudes which is actually only a function of the effective sample thickness due to higher Bragg orders, scattering background or sample inhomogeneity (Rabe et al 1979a).

In the next section we briefly describe our experimental setup.

In the following section the techniques to evaluate the three-dimensional arrangement of the atoms in the crystal are discussed in detail. Finally we compare our results with published X-ray diffraction data.

## 2. Experiment

The absorption spectra have been measured at the Deutsches Elektronen-Synchrotron (DESY) in Hamburg. Due to the finite source and exit slit size the degree of polarization of the synchrotron radiation amounts to at least 91%. This value is further increased by the crystal monochromator. In our experiment we used a channel-cut Si(220)-crystal with  $2d = 3.820 \text{ \AA}$ . The two Bragg reflections at the crystal slabs lead to a total calculated polarization of 94% at the sample. In the following discussion we shall neglect the small component with the electric vector perpendicular to the horizontal plane. The monochromatic radiation is monitored with two argon filled ionization chambers. Details about the experimental setup are subject of a forthcoming paper (Rabe et al 1979a).

A several  $\mu\text{m}$  thick sample was drawn from a bulk GeS single crystal by adhesive tape. It was oriented after a Laue pattern using a conventional X-ray tube. The b-axis was aligned parallel to the direction of the X-ray beam. The a-axis has been chosen to be parallel and perpendicular to the electric vector. The uncertainty for the alignment amounts to  $3^\circ$  for all axes. To reduce influences of thermal vibrations of the atoms on the amplitudes of the EXAFS the sample was cooled to liquid nitrogen temperature.

### 3. Results and discussion

The absorption spectrum for  $\vec{e} \parallel \vec{a}$  in the range of the Ge K-edge is shown in Fig. 1. The structure right at the edge does not show any anisotropy. This white line which probably is caused by density of states effects is omitted in the following data analysis.

Including the polarization dependence the fine-structure which extends to about 1.000 eV beyond the edge can be described by

$$(1) \quad \chi(k) = -\frac{1}{k} \sum_i A_i(k) P_i \sin(2kR_i + \bar{\Phi}_i(k))$$

where the sum runs over all scattering atoms surrounding the absorbing Ge atoms. The wavenumber  $k$  of the electron wave is calculated from the photon energy  $h\nu$  and some reference energy  $E_0$  through

$$(2) \quad k = (2m/h^2 (\hbar\nu - E_0))^{1/2} .$$

The periodicity of the EXAFS oscillations is determined by the bond lengths  $R_i$  between absorbing and scattering atoms and the phase  $\bar{\Phi}_i(k)$  the  $k$  dependence of which is characteristic for this atom pair.

The amplitude function is given by

$$(3) \quad A_i(k) = \frac{1}{R_i^2} |f_i(i, k)| \exp(-2R_i/r) \exp(-2\sigma_i^2 k^2) .$$

The  $k$  dependence of  $A_i(k)$  is mainly determined by the backscattering amplitude  $|f_i(i, k)|$  which in contrast to  $\bar{\Phi}_i(k)$  is a property of the scattering atom only. Differences in  $f_i(i, k)$  for different

atoms can be used to identify the scattering atom as we shall see later. An additional  $k$ -dependence in  $A_i(k)$  is caused by the distribution of the atoms around their equilibrium positions due to thermal vibrations. This disorder is expressed by a Debye-Waller factor with mean square relative displacements  $\sigma_i^2$ . The second exponential considers the damping of the electron wave by inelastic scattering processes through a mean free path  $\lambda$ .

For K-edge absorption the anisotropy of  $\chi(k)$  is introduced by

$$(4) \quad P_i = 3(\hat{R}_i \cdot \hat{e})^2 .$$

This term describes the orientation of the crystal ( $\hat{R}_i$  is the unit vector, pointing from the absorbing atom to the scatterer) relative to the electric vector  $\vec{e}$ . For isotropic samples or samples with cubic symmetry  $P_i$  can be replaced by the number of atoms  $N_i$  at the distance  $R_i$  and the sum in equ. 1 runs over all coordination spheres surrounding the absorbing atom.

From the absorption spectra the fine-structures  $k \cdot \chi(k)$  have been extracted by a procedure described in detail elsewhere (Martens et al 1978, Rabe 1978). The resulting EXAFS spectra for  $\vec{e} \parallel \vec{a}$  and  $\vec{e} \parallel \vec{c}$  are shown in Fig. 2. In these spectra the statistical noise has been eliminated by a Fourier filtering. This technique consists of a Fourier transformation of  $\chi(k)$  to real space and a subsequent inverse transformation to  $k$ -space after truncating the Fourier transform  $F(r)$  at  $r = 6\text{\AA}$ . This means that the high frequency components in  $k$ -space which show up at large  $r$  values in real space have been removed from the experimental spectra.

The two  $k \cdot \chi(k)$  spectra show significant difference in the whole  $k$  range. In the case of  $\vec{r} \parallel \vec{a}$  we observe a more rapid damping of the EXAFS at high  $k$  values compared to the  $\vec{r} \parallel \vec{c}$  spectrum. This is the first crude hint about relative contributions from different scattering atoms. As we shall see later the Ge scattering atoms lead to the dominant contribution to  $\chi(k)$  at large  $k$  values.

A quantitative analysis of these spectra is possible in real space. In Fig. 3a and 3b we show the magnitudes of the Fourier transforms  $|F(r)|$ , i.e. the direction dependent radial structure functions. These  $|F(r)|$  have been calculated by weighting  $k \cdot \chi(k)$  with a Gaussian window function which reaches 1/10 of its maximum value at the boundaries of the transformed  $k$  range ( $1.7\text{\AA}^{-1} \leq k \leq 12\text{\AA}^{-1}$ ). The effect of this window is a significant reduction of truncation effects in  $F(r)$ . A slight broadening of the structures in real space caused by the effectively reduced  $k$ -range has been tolerated.

In both cases a similar peak shows up at  $2\text{\AA}$ . The amplitude of this peak increases by 20% in going from  $\vec{r} \parallel \vec{a}$  to  $\vec{r} \parallel \vec{c}$ . At larger distance the structures differ significantly. The peaks in  $|F(r)|$  do not appear at the positions expected from the geometrical structures. They are shifted by the  $k$ -dependent parts of the scattering phase  $\phi_i(k)$  to smaller values compared to the true distances. This shift is characteristic for the absorber and scatterer pair. It can be evaluated from EXAFS spectra of reference samples with known interatomic distance as shall be discussed later.

From these radial structure functions we can directly get some information about the three-dimensional arrangement of the atoms in the

crystal. The magnitude of the Fourier transform is directly proportional to the polarization factor

$$(5) \quad (\hat{k} \cdot \hat{r})^2 = \cos^2(\alpha + \theta) \cos^2 \gamma.$$

The definition of the angles  $\alpha$  and  $\gamma$  is shown in Fig. 4 where the absorbing atom is located at A, the scattering atom at B. The angle between  $a$ -axis and polarization vector is denoted by  $\theta$ . From the ratio of the amplitudes of the first peak we obtain a value of  $\alpha = 47^\circ \pm 1^\circ$ . The second peak at  $2.8\text{\AA}$  in  $|F(r)|$  for  $\vec{r} \parallel \vec{a}$  is reduced by about a factor of 3 in going to  $\vec{r} \parallel \vec{c}$  from which we calculate  $\alpha = 30^\circ \pm 5^\circ$ . From the fact that almost no contribution to  $|F(r)|$  for  $\vec{r} \parallel \vec{a}$  is observed at  $3.3\text{\AA}$  we conclude that the prominent structure at this distance in the case  $\vec{r} \parallel \vec{c}$  is caused by scattering atoms with  $\alpha = 90^\circ \pm 5^\circ$ . The relatively large errors in the last two cases had to be introduced because contributions from strong neighbouring peaks may influence the amplitude of the central peak. We have summarized these values in table 1. A comparison with angles derived from X-ray diffraction data (Bissert and Besse 1978) shows the excellent agreement with our result. It should be noted that these angles are not uniquely defined from our experiment. As we measured  $\chi(k)$  only for the two values  $\theta = 0^\circ$  and  $\theta = 90^\circ$  we cannot determine the sign of  $\alpha$ . Furthermore inspecting eq. 5, the angles  $\alpha$  and  $\alpha + 180^\circ$  are equivalent and therefore lead to the same EXAFS in general. No information can be extracted from our data about the angle  $\gamma$ . In principle this would be possible from an experiment where the sample has been rotated around the vertical axis.

An identification of the type of scattering atom is possible through the shape of the amplitude-function  $A(k)$  (Rabe et al 1979b). Apart from the monotonous Debye-Waller factor the  $k$ -dependence of  $A(k)$  is determined by the backscattering amplitude  $|f(q,k)|$ . The amplitude function of the first isolated scattering shell calculated from the inverse Fourier transform carried out over the range as indicated by a bar in Fig. 3b is shown in Fig. 5. It has the typical shape of a light element. The  $A(k)$  of Ge calculated in the same way from the EXAFS of pure crystalline Ge is included in Fig. 5. Whereas  $A_S(k)$  shows large amplitudes at small  $k$ -value and decreases monotonously to higher  $k$ -values,  $A_{Ge}(k)$  has a maximum at  $k \approx 5 \text{ \AA}^{-1}$ . These differences can be used for an identification of the scattering atoms at larger distances from the absorbing atom. A reduction of the transformation range from  $1.7 \text{ \AA}^{-1} \leq k \leq 12 \text{ \AA}^{-1}$  to  $5 \text{ \AA}^{-1} \leq k \leq 12 \text{ \AA}^{-1}$  should lead to a significant reduction of structures in  $|F(r)|$  attributed to S-scattering atoms whereas peaks attributed to Ge shells should be almost unchanged. The results of this Fourier transform are shown in Fig. 3c and 3d. The  $|F(r)|$  from Fig. 3a and 3b have been included for comparison. The amplitudes of the first two structures in  $|F(r)|$  for  $\vec{a}$  and  $\vec{b}$  are reduced significantly as expected for S-scattering atoms. On the other hand the amplitude and the shape of the peak around  $3.8 \text{ \AA}$  is almost unchanged. Therefore this structure has to be attributed to Ge scatterers. The asymmetry points to the fact that more than one shell of Ge atoms yield comparable contributions to this structure.

A similar effect in the magnitude of the Fourier transform can be expected from a different weighting of the fine-structure  $\chi(k)$ . The radial structure functions in Fig. 3a-d have been obtained

from a Fourier transform of  $k\chi(k)$ . A Fourier transform over  $k^3\chi(k)$  in the range  $1.7 \text{ \AA}^{-1} \leq k \leq 12 \text{ \AA}^{-1}$  (same as for Fig. 3a and 3b) emphasizes the amplitude function  $A(k)$  at large  $k$ -values, i.e. favours the contribution from Ge atoms. Fig. 3e and 3f show the result. As expected the Ge attributed structures have increased compared to the S peaks.

To explain the differences in the radial structure functions we have made a graphic comparison of our experimental  $|F(r)|$  with the crystal structure data of GeS derived from X-ray diffraction experiments (Bissert and Hesse 1978). The bondlengths  $R_i$  between absorbing and scattering atoms, the angles  $\alpha$  and  $\gamma$  (eq. 5), and the coordination numbers  $n_i$ , i.e. the number of atoms with the same values  $\cos^2\alpha$ ,  $\cos^2\gamma$  and  $R_i$  are listed in table 1. The different scattering shells have been symbolized by vertical solid (S scattering atoms) and dashed (Ge scattering atoms) bars in Fig. 3.

For this comparison the peak position (represented by the position of the bars) and the peak amplitudes (represented by the lengths of the bars) in  $|F(r)|$  had to be calculated. The difference between the position of the first peak in  $|F(r)|$  for  $\vec{c}$  and the bondlength  $R_1 = 2.42 \text{ \AA}$  of this shell yields the shift of  $0.44 \text{ \AA}$  for all bars representing the S atoms. The shift of the bars attributed to Ge atoms ( $0.30 \text{ \AA}$ ) has been taken from a radial structure function of crystalline Ge (Rabe et al 1979c) calculated from a Fourier transform of the Ge K-shell EXAFS over the same  $k$ -range as in the case of GeS. An excellent agreement between the peak positions in  $|F(r)|$  and positions calculated from the recent X-ray diffraction results is observed.

The amplitudes of the peaks have been calculated from

$$(6) \quad U_i = 3 (\hat{R}_i \cdot \hat{r})^2 \frac{n_i}{R_i^2} \exp(-2R_i/\lambda) E_i$$

The weighting factor  $E_i$  considers the influence of differences in  $|f_i(q, k)|$  for the different atomic species, S and Ge, on the amplitudes of peaks in  $|F(r)|$ . In detail the values for the  $E_i$  have been determined in the following way: i)  $E_{Ge}$  has been calculated from  $|F(r)|$  of crystalline Ge which was obtained from a Fourier transform of the EXAFS over the same spectral ranges using the same transformation windows as used in the case of GeS.  $E_S$  has been taken from the first structure of  $|F(r)|$  of GeS for  $\vec{c} \parallel \vec{c}$ . The actual height of the peaks in  $|F(r)|$  also depends on the Debye-Waller factors (cf. eq. 3) which are unknown for the  $i = 2$  neighbours. Therefore differences in the  $n_i^2$  have not been taken into account in the  $E_i$ . ii) For  $\lambda/a$  value of  $6\text{\AA}$  has been used. iii)  $(\hat{R}_i \cdot \hat{r})^2$  has been calculated from eq. 5 using the angles  $\theta$  and  $\phi$  listed in table 1. Depending on the direction of the polarization vector between seven ( $\vec{c} \parallel \vec{c}$ ) and eleven ( $\vec{c} \parallel \vec{a}$ ) shells of atoms in the spacial range  $0 < r < 5\text{\AA}$  yield contributions to the EXAFS. According to this complicated structure only the nearest neighbours are resolved completely. Nevertheless the overall agreement of the peak heights between the experimental  $|F(r)|$  and the calculated radial structure is quite satisfactory.

For the second S shell at  $r = 2.7\text{\AA}$  the amplitude seems to be overestimated by the calculation. This fact is probably due

to variations of the correlation of the atomic motion with direction and radial distance resulting in different  $n_i^2$  for different  $i$  (Goni and Plateman 1976, Böhmér and Rabe 1979). Especially in strong covalent bonds the nearest neighbour motions are known to be highly correlated and large differences are expected between nearest and next nearest neighbours (Rabe et al 1979c). Using the backscattering amplitude  $f(i, k)$  for S calculated by Teo and Lee (1979) we have determined the mean square relative displacement  $\sigma^2$  for the nearest neighbours from the slope of a plot of  $\ln(A(k)/|f(i, k)|)$  versus  $k^2$ . The result is  $\sigma^2 = (8.3) \cdot 10^{-4}\text{\AA}^2$ . To account for the decreased amplitude of the second peak an additional  $\sigma^2$  of approximately  $5 \times 10^{-3}\text{\AA}^2$  has to be used.



#### 4. Conclusion

The good agreement of the anisotropic EXAFS results with X-ray diffraction data shows the feasibility of direction dependent structure studies by EXAFS with polarized radiation. Clearly the various well established diffraction techniques will usually be favoured for systems with long range periodic order. Nevertheless EXAFS directly yields partial pair correlation functions for the surrounding of the absorbing atom which may be useful for the interpretation of diffraction data. Additionally the anisotropic EXAFS can yield valuable structure information about oriented samples, which are not available as perfect crystals in the sense of X-ray diffraction.

#### Acknowledgements

We would like to thank Ch. Nissen for orienting the GeS crystal. The support of Prof. R. Haensel is gratefully acknowledged. We thank B.-K. Tee and P. Lee for informing us of their theoretical results prior to publication. This work was financially supported by the Bundesministerium für Forschung und Technologie BMT.

#### References

- Beni G, Platzman P M, 1976, Phys.Rev. B14, 1514-1518
- Bissert G and Hesse K F, 1978, Acta Cryst B34, 1322-1323
- Böhm W and Rabe P, 1979, J.Phys. C12, 2465-2474
- Brown G S, Eisenberger P, and Schmidt P, 1977, Solid State Commun 24, 201-203
- Heald S M and Stern E A, 1977, Phys.Rev. B16, 5549-5559
- Heald S M and Stern E A, 1978, Phys.Rev. B17, 4069-
- Lytle F W, Sayers D E, and Stern E A, 1975, Phys.Rev. B11, 4825-4835
- Martens G, Rabe P, Schwentner N, and Werner A, 1978, Phys.Rev. B17, 1481-1488
- Parratt L G, Hempstead D F, and Jossem E L, 1957, Phys.Rev. 105, 1228-1232
- Rabe P, 1978, Jap.J.Appl.Phys. 17-2, 22-29
- Rabe P, Tolkieln G, and Werner A, 1979a, submitted to Nucl.Instr. and Methods
- Rabe P, Tolkieln G, and Werner A, 1979b, J.Phys. C12, 899-905
- Rabe P, Tolkieln G, and Werner A, 1979c, J.Phys. C12, 1545-550
- Rehr J J, Stern E A, Martin R L, and Davidson E R, 1978, Phys.Rev. B17, 560-565
- Stern E A, 1974, Phys.Rev. B10, 3027-3037
- Stern E A, Sayers D E, and Lytle F W, 1975, Phys.Rev. B11, 4836-4846
- Tee B K and Lee P A, J.Am.Chem.Soc. 101, 1979, 2815-2832
- Wyckoff R W, 1968, Crystal Structures, Vol.1 (New York: Interscience Publishers)

Table caption

Table 1: Bondlengths  $R_1$  between central Ge and scatter, angles  $\alpha$  and  $\gamma$  defined in Fig. 4, coordination number  $n_1$  and type of scatterer as determined by X-ray diffraction (Bissert and Hesse 1978) and by EXAFS.

Figure captions

Fig. 1: Absorption spectrum of GeS at the Ge K-edge for the electric vector  $\vec{E}$  parallel  $\vec{a}$ .

Fig. 2: Fourier filtered finestructures  $k \cdot \chi(k)$  for  $\vec{a}$  parallel  $\vec{a}$  and  $\vec{E}$  parallel  $\vec{c}$ .

Fig. 3: Magnitude of the Fourier transform  $|\hat{F}(r)|$  calculated from  $\chi(k)k^n$  with a Gaussian window function and different transformed  $k$ -ranges.

a) and b)  $1.7\text{\AA}^{-1} < k < 12\text{\AA}^{-1}$ ,  $n = 1$ ;

c) and d)  $5\text{\AA}^{-1} < k < 12\text{\AA}^{-1}$ ,  $n = 1$ ;

e) and f)  $1.7\text{\AA}^{-1} < k < 12\text{\AA}^{-1}$ ,  $n = 3$ .

Fig. 4: Definition of the angles  $\alpha$  and  $\gamma$  used in text.

Fig. 5: Experimental amplitude functions  $A(k)$  for Ge and S scatterers calculated from an inverse Fourier transform.

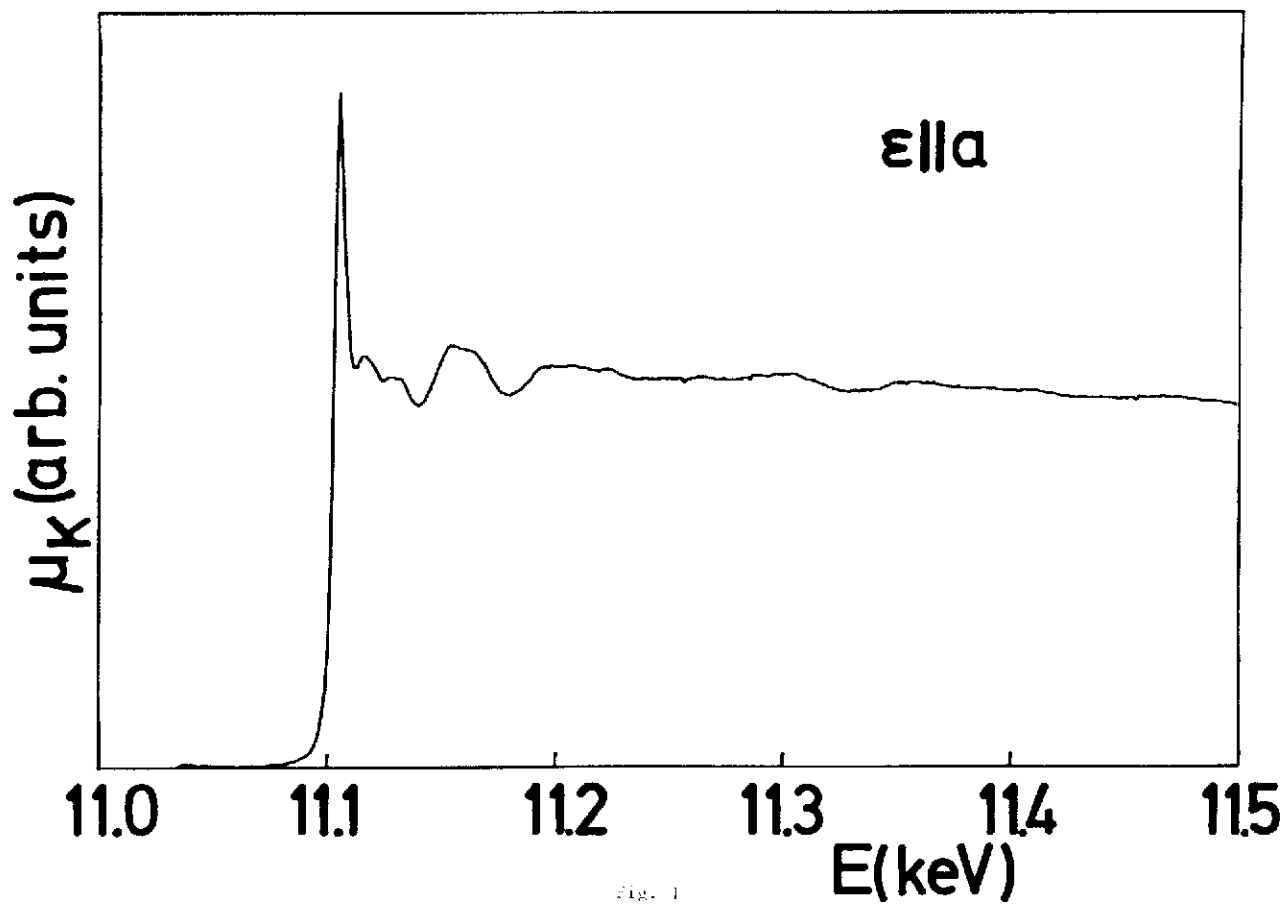


Table 1

$R_i$ [ $\text{\AA}$ ]	$\theta$ [deg]		$r$ [deg]	$n_i$	element	
	diff.	EXAFS			diff.	diff.
2.4407	0		76.97	1	S	
2.4414	48.72	47 $\pm$ 1	7.11	2	S	S
3.269	34.0	30 $\pm$ 5	5.30	2	S	S
3.278	0		60.64	1	S	
3.322	59.05		50.28	2	Ge	
3.641	90	90 $\pm$ 5	0	2	Ge	Ge
3.887	40.28		43.58	4	Ge	
3.924	0		46.73	1	S	
4.297	0	0 $\pm$ 10	0	2	Ge	Ge
4.384	81.41		32.85	2	S	
4.4377	0		32.4	1	S	
4.4852	29.60		34.73	2	Ge	
4.8991	66.18		35.67	2	S	

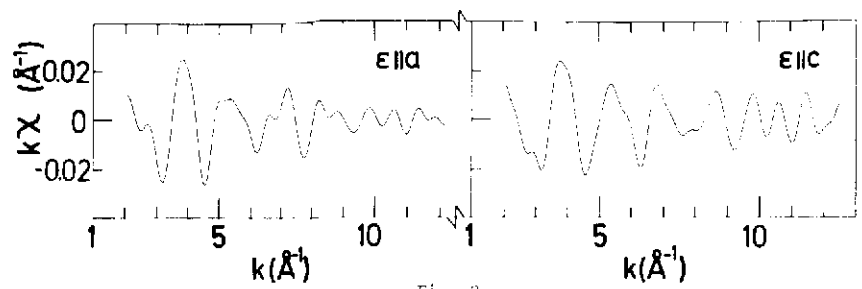


Fig. 2

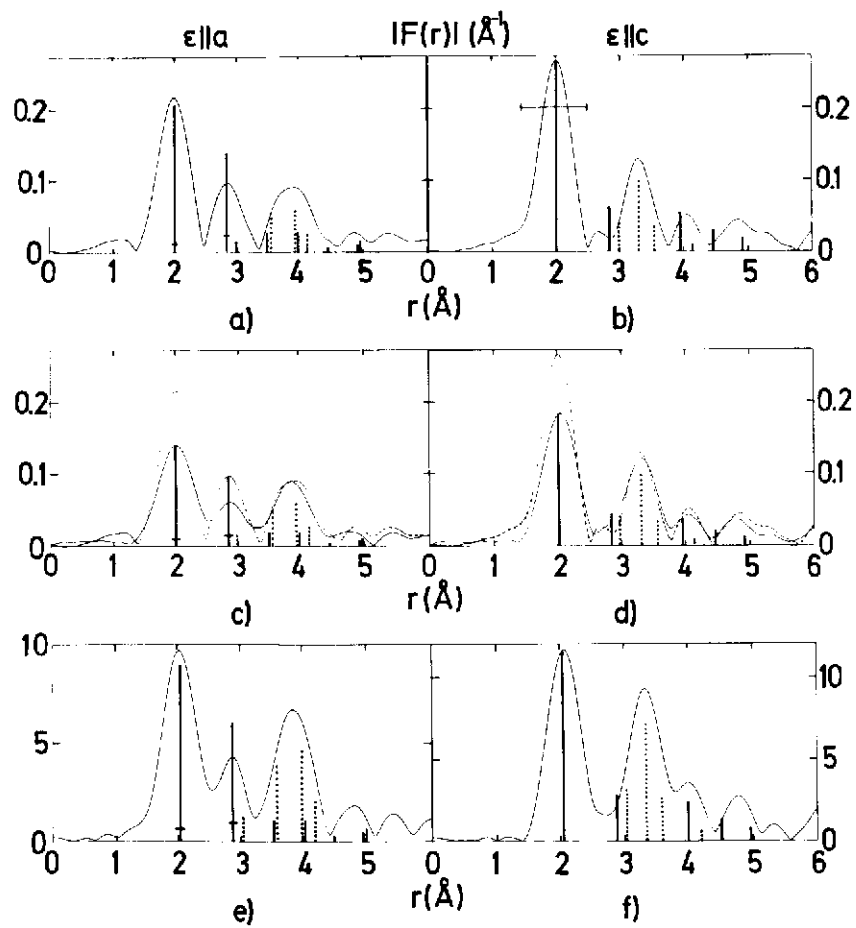


Fig. 3

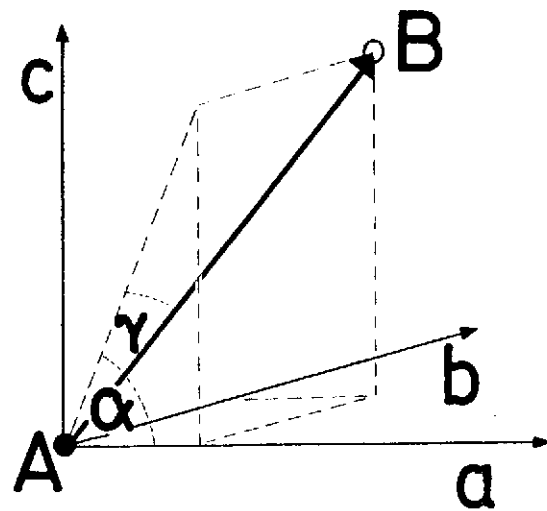


Fig. 4

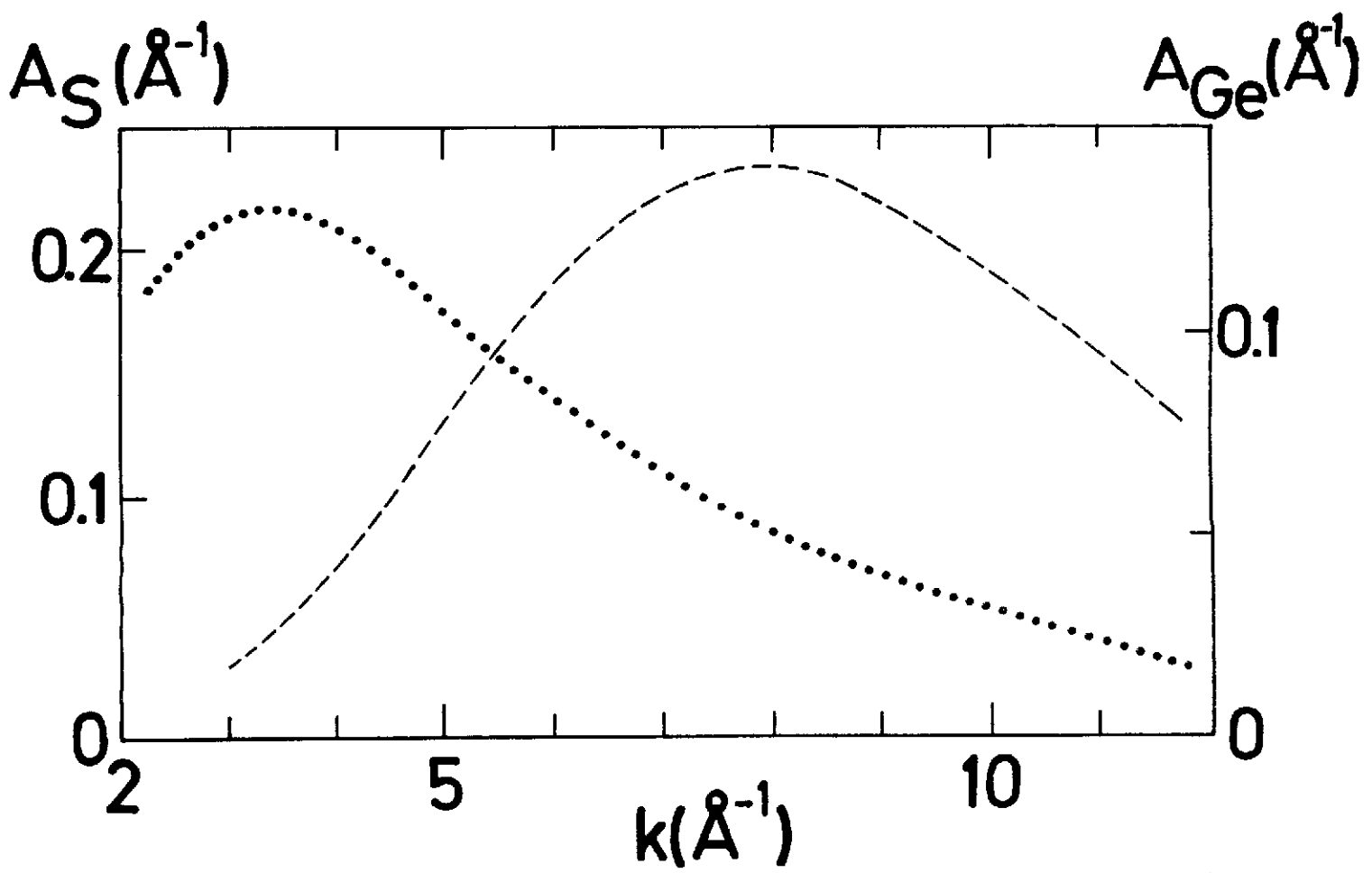


Fig. 5